GEOPHYSICAL RESEARCH LETTERS, VOL. 16, NO. 12, PAGES 1417-1420, DECEMBER 1989

REGIONAL ANALYSIS OF D" VELOCITIES FROM THE RAY PARAMETERS OF DIFFRACTED *P* PROFILES

Michael E. Wysession and Emile A. Okal

Department of Geological Sciences, Northwestern University, Evanston, Illinois

Abstract. In examining the slownesses of linear profiles of diffracted *P* arrivals, we have discerned regional variations in the compressional velocity structure of D", the base of the mantle. Three methods of determining the slownesses were tested, concluding that the waveform cross-correlation (XC) technique is more reliable over a wide range of epicentral distances than methods involving a linear regression through either the first motion or first peak arrival times. XC slownesses suggest a statistically conservative range in D" average velocities of 3.1%, and reveal regions of very fast velocities under Asia and the eastern Pacific basin and of very slow velocities under the New Guinea/Solomon Islands region. Slownesses were found to correlate well with the tomographic model V3 of *Morelli and Dziewonski* [1986], derived from a different technique and data set. Synthetic seismograms were generated using a summation of spheroidal normal modes, and at periods greater than 45 s the diffracted waves show much less variation and are very well modeled by PREM.

Introduction

Chemical and/or thermal differences in the structure of D" have recently been detected with a diverse array of techniques in the fields of seismology, geomagnetics, geodesy, geothermometry and geodynamics. Together with advances in mineral physics, these efforts have given us greater insight as to the processes shaping D". These lateral heterogeneities have been quantified by seismologists using both global studies with tomographic inversions of many travel times, and regional studies involving a closer examination of fewer teleseismic arrivals. Diffracted waves (*Pd*, *Sd*) have been a popular choice for the latter.

In *Wysession and Okal* [1988, "Paper I"], we compared slownesses across profiles of *Sd* arrivals to those of synthetic *Sd* pulses, and constructed a limited map of shear velocities (V_S) in D". We found a 3.5% variation in slowness (hence in V_S) with our coverage, and verified that a high V_S zone in the manner of *Lay and Helmberger* [1983] was appropriate in modeling D" beneath the NE Pacific plate boundary. In order to get a better understanding of the elastic properties of the base of the mantle, we now extend these techniques to velocities V_P in D". Because the translation of apparent ray parameters (p_a) into velocities is not simple [Paper I; *Mula and Müller*, 1980; *Aki and Richards*, 1980], two approaches can be taken toward interpretation: compare regions of the CMB only by their slownesses, in terms of relative velocity perturbations, or create synthetic seismograms of the arrivals, determine their slowness and then compare this to the data p_a, thus deriving in absolute terms the goodness of the model at simulating the data. Both approaches are taken here.

Paper number 89GL03443.
0094-8276/89/89GL-03443$03.00

Data and Corrections

We use 140 long period vertical WWSSN and Canadian records from 13 large ($m_b \geq 5.9$) earthquakes. Several of those have been previously studied, in particular by *Mula and Müller* [1980]. We restrict ourselves to 20 independent azimuthally narrow profiles of the *Pd* arrivals, ranging in epicentral distance Δ from 99 to 161°. Although the *Pd* signals are small at greater distances, they are often clear, being the first arrivals. Events are listed in Table 1, and profiles in Table 2, arranged by CMB region.

Our regional coverage of D" was controlled by certain criteria regarding station configurations along profiles, and by the limited distribution of large post-1962 earthquakes. To ensure a reliable determination we require a minimum distance range along the CMB of 15°. We also tried to use at least 4 stations in a profile, averaging 6 per path. We restricted the azimuthal range to a maximum of 18°, (with a path average of 11.6°), both to allow sampling of a continuous path through D" and to avoid travel time delays due to source effects and slab diffraction along the *Pd* downswing [*Cormier*, 1989]. Deep events gave clear arrivals for *Pd* and its surface reflections, *pPd* and *sPd*, but our narrow azimuthal windows also allowed us to use shallow events, for though these arrivals are a combination of all 3 pulses, at a given azimuth all signals still leave the source with the same waveshape. Figure 1 shows an example of our data.

Travel times were corrected for both ellipticity and the upswing paths through the heterogeneous mantle and crust. Ellipticity corrections ranged from -1.15 to +1.07 s, often differing by more than 1 s for arrivals along a single profile. Each upswing path being through a different part of the mantle, we wanted to correct them by using a tomographic model of V_P perturbations in the mantle. Since a full-mantle V_P model is not currently available, we had the choice of using the spherical harmonic coefficients from a full-mantle V_S model or combining a lower mantle V_P model with an upper mantle V_S model. For the sake of consistency with our *Sd* study we use the full-mantle and crust V_S coefficients of Woodhouse (pers. comm., 1989), and scale it appropriately for V_P, assuming $d(lnV_P)/d(lnV_S) = 0.5$. The range in corrections for our data was

TABLE 1. Events Used for This Study

Event No.	Location	Date M/D/Y	Origin Time	Epicenter (°N)	Epicenter (°E)	Depth (km)	m_b
1	Taiwan	2/13/63	0850:05	24.41	122.09	53	6.2
2	Peru	8/15/63	1725:11	-13.78	-69.26	593	6.0
3	Brazil	11/9/63	2115:30	-8.83	-71.67	576	5.9
4	So. Sandwich	9/14/66	2318:42	-60.33	-27.25	27	5.9
5	Sumatra	5/21/67	1845:13	-0.96	101.39	184	6.2
6	Sumatra	8/21/67	0733:02	3.72	95.74	40	6.1
7	Tonga	10/9/67	1721:46	-21.10	-179.20	605	6.2
8	Nicaragua	10/15/67	0800:53	11.91	-85.98	181	6.2
9	Kermadec	7/25/68	0723:02	-30.97	-178.13	17	6.5
10	Borneo	8/10/68	0207:00	1.38	126.24	1	6.3
11	Tonga	2/10/69	2258:03	-22.75	178.76	635	6.0
12	Kermadec	3/30/72	0534:50	-25.69	179.58	479	6.1
13	N. Korea	9/29/73	0044:00	41.93	130.99	567	6.3

TABLE 2. CMB Path Profile Data and Results for This Study

Event. Profile	CMB Path Description	No. of Sta.	Distance Range (°)	Azimuth Range (°)	Slownesses XC	PM	FM
			Full Profiles				
1.1	Taiwan to S. America	6	112-145	6-16	4.55	4.50	4.44
1.2	Taiwan to S. America	5	100-147	20-31	4.64	4.56	4.55
1.3	Taiwan to S. America	7	100-149	31-42	4.62	4.58	4.52
13.1	N. Korea to S. America	8	113-155	32-53	4.64	4.62	4.54
2.1	Peru to South Asia	4	101-159	54-59	4.64	4.69	4.57
3.1	Brazil to South Asia	7	100-157	50-62	4.62	4.55	4.52
8.1	Nicaragua to South Asia	5	100-144	34-50	4.61	4.56	4.52
4.1	So. Sandwich to N. America	10	104-129	297-314	4.60	4.51	4.52
4.2	So. Sandwich to N. America	10	107-113	318-329	----	4.53	4.26
5.1	Sumatra to N. America	6	100-144	24-35	4.61	4.60	4.59
6.1	Sumatra to N. America	5	120-136	27-33	4.60	4.55	4.34
10.1	Borneo to N. America	7	107-157	25-37	4.57	4.53	4.50
10.2	Borneo to Europe	7	102-133	321-332	4.51	4.44	4.44
7.1	Tonga to N. America	8	102-123	50-58	4.55	4.57	4.49
9.1	Kermadec to N. America	6	109-128	56-62	4.51	4.53	4.42
12.1	Kermadec to N. America	6	105-121	55-63	4.49	4.45	4.57
9.2	Kermadec to Europe	6	113-157	12-23	4.55	4.54	4.54
7.2	Tonga to Mid-East (whole)	6	111-148	291-303	4.54	4.51	4.54
11.1	Tonga to Mid-East (whole)	7	110-147	290-302	4.54	4.54	4.50
9.3	Ker. to Mid-East (whole)	8	116-161	280-296	4.61	4.53	4.51
12.2	Ker. to Mid-East (whole)	8	99-148	287-297	4.59	4.55	4.58
			Partial Profiles				
7.2a	Tonga to Mid-East (1st part)	3	111-127	293-300	4.67	4.63	4.64
11.1a	Tonga to Mid-East (1st part)	4	110-126	293-299	4.70	4.69	4.59
9.3a	Ker. to Mid-East (1st part)	4	116-132	287-292	4.80	4.77	4.69
12.2a	Ker. to Mid-East (1st part)	5	99-121	291-296	4.65	4.65	4.66
7.2b	Tonga to Mid-East (2nd part)	4	127-148	291-303	4.47	4.50	4.52
11.1b	Tonga to Mid-East (2nd part)	4	126-147	290-302	4.52	4.56	4.47
9.3b	Ker. to Mid-East (2nd part)	5	132-161	280-296	4.51	4.45	4.45
12.2b	Ker. to Mid-East (2nd part)	5	120-148	287-297	4.53	4.49	4.53

-0.81 to +1.23 s. Individually they resulted in maximum changes to the slownesses of only 0.04 and 0.03 s/° respectively (e.g., from 4.59 to 4.63 s/°), and combined had an average magnitude of change of 0.015 s/°, or only 0.3%.

Procedure

Three different techniques have previously been used to determine the apparent ray parameter of a profile of diffracted arrivals: first motion onsets (FM), first peak maxima (PM), and waveform cross-correlation (XC).

First motions. Traditionally these have been picked and a slope fit through them with a linear regression. While the first motion onsets may be controlled by V_P only a few tens of kilometers into D" [*Bolt and Niazi*, 1984], this method has the disadvantage that arrivals are often emergent, and errors involved with choosing an onset time can be on the order of several seconds.

First peaks. A linear regression can also be done with the arrival times of the first peak maxima [*Mondt*, 1977; *Mula and Müller*, 1980]. This has the advantage of being an easily chosen time (though peaks are occasionally complicated by noise), but it becomes unclear what the slowness actually represents, leading *Mula and Müller* [1980] to call it an apparent ray parameter.

Cross-correlations. The third method, used in Paper I, involves a multiple cross-correlation of the windowed diffracted waveforms, with the slowness found by the peak of the XC function. This method is much less sensitive to noise, and also allows for a direct comparison with synthetic seismograms, which we have generated using a summation of normal modes. This method is lower-frequency, and thus the slowness is controlled by a thicker portion of D". Like the PM method, it is affected by the waveform's change in frequency with Δ. The XC method is most sensitive to frequencies with the greatest energy, and we clearly observe in all of our *Pd* profiles a spectral shift toward lower frequencies with increased Δ.

Thus, for a given profile, we both expect and observe these 3 methods to give different values as the waveforms widen at greater Δ, with the FM method giving the lowest value, the PM one a slightly higher value and the XC one the highest value. Combining 28 profiles, slowness averages were: 4.527 ± 0.074 s/° (FM), 4.559 ± 0.076 s/° (PM), and 4.587 ± 0.072 s/° (XC). As confident indications of the range of V_P sampled in D", these standard deviations σ would imply lateral variations at the CMB of 3.3%, 3.3% and 3.1% respectively. Despite the similarities

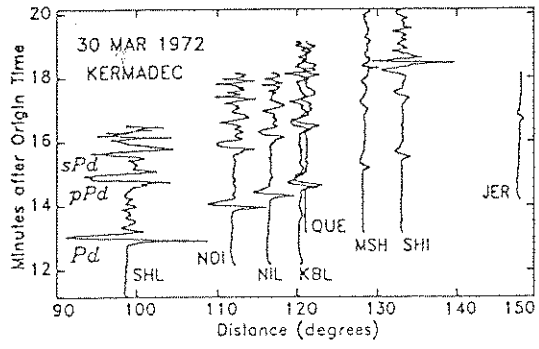

Fig. 1. Example of profile (12.2) of *Pd*, *pPd*, and *sPd* arrivals. Records have been equalized to a common gain.

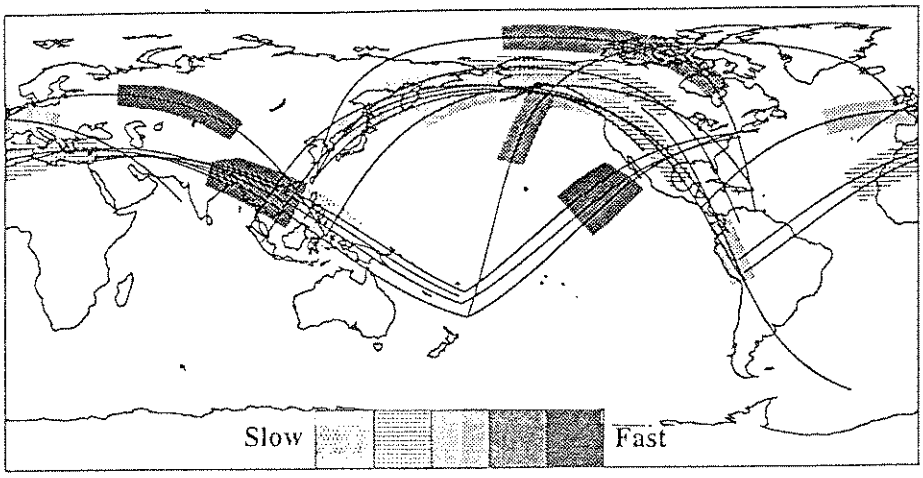

Fig. 2. Relative values of V_P in D", mapped from our XC-determined slownesses, and projected onto the Earth's surface. Solid curves are average paths, and shaded areas the sampled D" regions.

in σ, there were differences in the reliability of the 3 methods. The FM method seemed least reliable. It had consistently higher χ^2 from the linear regressions than did the PM method for the same station geometries. Also, while the XC and PM methods correlated together well between similar profile slownesses (correlation coefficient R = 0.88), the FM method did not correlate as well with either of the other two methods: $R = 0.62$ for FM-XC, and $R = 0.64$ for FM-PM. All 3 methods had very small statistical errors for profiles covering a long range of Δ, but sensitivities differed for small ranges. An example is profile 4.2 (not used in our calculations), adjacent to 4.1, and whose short range (Δ = 106.7–113.0°) made it unreliable even though it had 10 stations. There was no clear XC peak, and the FM slowness changed considerably: p_a = 4.52 ± 0.04 s/° for profile 4.1, and 4.26 ± 0.13 s/° for 4.2. Only the PM slowness seemed consistent (p_a = 4.51 ± 0.04 s/° for 4.1, and 4.53 ± 0.13 s/° for 4.2). The standard deviations assume a ± 1 s error in picking arrival times, but the different results between the FM and PM methods imply that actual errors may be greater. Furthermore, the very slow V_S found by *Bolt and Niazi* [1984] using the FM method was for a profile of 9 arrivals, but spanning only 7° in Δ. Over such short ranges, FM may not be reliable to find a slowness, since p_a is already more affected by travel-time errors from localized small-scale heterogeneity.

For studying CMB diffracted waves, we consider the XC method to be superior. Arrivals well into the shadow zone are often emergent and of small amplitude, yielding lower signal to noise ratios; the XC method is the most stable in these cases, with PM running as second choice.

Observations

Figure 2 is a map of inferred relative core-mantle boundary P velocities, projected onto the earth's surface, based on our XC apparent ray parameters listed in Table 2. The lateral heterogeneity is evident. The range in slownesses is 4.47–4.80 s/°, a 7.1% lateral change in average V_P, though a better measure of the scatter may be our conservative estimate of 3.1%, based on a ± 1 σ deviation from the mean of the distribution of the 28 profiles.

We found two regions with very fast V_P (under the NE Pacific and Asia), and one with very slow V_P (under New Guinea/Solomon). The V_P high under the Pacific west of Mexico is seen in profiles 7.1, 9.1 and 12.1 from Tonga/Kermadec to North America. Their slownesses agree well and their mean (4.52 s/°) is much slower than our global average (4.59 s/°). The other high, located under Asia, is adjacent to the New Guinea/Solomon low. It is seen in profile 10.2 (Borneo to Europe; p_a = 4.51 s/°), and both the high and low are seen in the four profiles from Tonga/Kermadec to the Middle East (7.2, 11.1, 9.3 and 12.2). These long paths travel almost 50° along the CMB, and extend across the V_P high and low. Indeed, the slownesses of the full profiles (7.2, 11.1, 9.3, 12.2) are near average, but p_a for profiles sampling the first half (7.2a, 11.1a, 9.3a, 12.2a) averages 4.71 s/° (slowest in our study), while p_a for the second half (7.2b, 11.1b, 9.3b, 12.2b) averages 4.51 s/°, implying the fastest V_P in our study.

The slownesses of our other profiles are closer to the mean of our set. CMB velocities seem slightly slow beneath Northern Africa and the Mediterranean, but are average beneath the Northeast Atlantic and Europe. Implied V_P beneath Western South America are also average for our study, and with the many profiles from East Asia to the Americas and Europe we see a gradation from fast to slow, then to fast again as we traverse the CMB from beneath the North Pacific to the North Pole.

The correlation between these implied V_P and the V_S values found in Paper I is mixed. The Tonga to Mid-East path revealed the same high and low V_S anomalies when *Sd* profiles were reexamined and split. But implied V_S under the Eastern Pacific were only moderately fast (compared to very fast P velocities), and the fastest V_S were found under Northwest North America, where the current study implies slightly slower V_P .

However, correlations with some global tomographic models of V_P in D" are very good. For example, both model V3 [*Morelli and Dziewonski*, 1986] and that of *Inoue et al.* [1989] reflect the major V_P anomalies found here. They both find velocity highs under Asia and the East Pacific and a strong low under New Guinea/Solomon, with more average values in our average regions. The magnitude of the range in velocities found in D" by these two models is slightly less than in our study: ≈ 2% for *Inoue et al.*'s [1989] model and ≈ 1.5% for V3, compared to at least a 3% variation from this study's *Pd* slownesses.

To study the correlation of our results with the V3 model, we calculated the average velocity perturbations along all our paths using the spherical harmonic

coefficients of V3. The correlation between these average path velocities and our XC slownesses is good (R = -0.53). Correlations between these V3 path velocities and the other two methods were only R = –0.19 (FM) and –0.31 (PM).

In 6 instances, we had profiles of strong and distinct surface reflected *pPd* arrivals. The p_a for these profiles agreed extremely well with those of corresponding *Pd*, differing by an average of +0.03 and +0.02 s/° for the XC and PM methods (FM picks were unreliable). While these did not give us any new insight into D" structure, they did assure us that procedural errors were minimal, and in particular that we successfully avoided the potential problem of heterogeneity in the source region [*Cormier*, 1989].

Comparison with Synthetics

Up to now, we only discussed relative velocities – both with the apparent ray parameters of our *Pd* profiles and with the comparisons with global tomographic models. In an attempt to infer the absolute V_P of the regions sampled, we generated synthetic seismograms and calculated slownesses from their windowed pulses using the XC method. For a given profile of stations, the ability of our velocity structure to model the actual region depends on the closeness of the actual and synthetic p_a. We use the PREM structure of *Dziewonski and Anderson* [1981], and a summation of spheroidal normal modes simulating the frequency effects in the *Pd* waveforms. These synthetics are generated using exact fault parameters and event-station geometries for each arrival [*Kanamori and Cipar*, 1974].

Because of the ease in computing torsional modes, we used for *Sd* in Paper I all modes down to periods T = 20 s. Here, due to the complexity of overtone branches, we built *Pd* synthetics summing only modes with $T \geq$ 45 s. To compare with the data, we low-pass filter our observed *Pd* arrivals at 45 s, and compare XC slownesses. We were limited to profiles with long ranges in Δ because the lack of high frequencies caused greater uncertainty in our XC coefficients, but we also could not use arrivals at very large Δ, since *Pd* then precedes the much larger *PKP* by less than 2 mn, and the synthetic is contaminated by *PKP*.

Six profiles covering 3 distinct paths allowed for reliable comparisons, and we found that at $T \geq$ 45 s the data slownesses were both similar to each other and to the corresponding PREM values. Four of the profiles (7.2, 11.1, 9.3, 12.2) were along the Tonga/Kermadec to Mid-East path, with slownesses of 4.67, 4.67, 4.67 and 4.64 s/°. The other two profiles, Brazil–So. Asia, and Korea–So. America (3.1 and 13.1), had p_a = 4.69 and 4.64 s/°. Synthetic p_a differed on average by only 0.02 s/° from the corresponding data values. The similarities between the data are less than in the unfiltered data, and the slownesses are all greater (most likely because they sample mantle farther above the CMB and thus lower V_P). This suggests that much of the lateral heterogeneity in V_P is concentrated close enough to the CMB that 45 s *Pd* waves are not very affected by it. It also suggests that at these wavelengths PREM appropriately models *Pd* velocities.

Conclusions

Pd slownesses supply information about average V_P in D", through both relative comparisons between the data, and absolute comparisons to the slownesses of synthetics. Examination of *Pd* profiles from 13 large events have identified several regions of anomalous V_P along the CMB. Most notable are the V_P highs under Asia and the East Pacific Basin, and the V_P low under the SW Pacific. This range suggests statistically significant lateral variations in V_P in D" of at least 3.1%. Corrections for ellipticity and upswing path mantle heterogeneity were of an order of magnitude less than this variation. Comparison with synthetics reveals that at longer wavelengths path slownesses are well modeled by a PREM structure.

Acknowledgements. We thank A. Morelli for the use of the unpublished model V3, and J. Woodhouse for his unpublished full-mantle S velocity model. This work was supported in part by NSF grant EAR-84-05040.

References

Aki, K., and P.G. Richards, *Quantitative Seismology*, W.H. Freeman, San Francisco, 932 pp., 1980.

Bolt, B.A., and M. Niazi, S velocities in D" from diffracted SH-waves at the core boundary, *Geophys. J., 79,* 825-834, 1984.

Cormier, V.F., Slab diffraction of S waves, *J. Geophys. Res., 94,* 3006-3024, 1989.

Dziewonski, A., Mapping the lower mantle: determination of lateral heterogeneity in P velocity up to degree and order 6, *J. Geophys. Res., 89,* 5929-5952, 1984.

Dziewonski, A., and D.L. Anderson, Preliminary reference Earth model, *Phys. Earth Plan. Int., 25,* 297-356, 1981.

Inoue, H., Y. Fukao, K. Tanabe and Y. Ogata, Whole Mantle P-Wave Travel Time Tomography (abstract), *Proc. XXV Gen. Assemb. IASPEI, Istanbul,* p. 73, 1989.

Jeffreys, H., and K.E. Bullen, *Seismological tables,* Brit. Assoc. Adv. Science, London, 50 pp., 1970.

Kanamori, H., and J.J. Cipar, Focal process of the great Chilean earthquake, *Phys. Earth Plan. Int., 9,* 128-136, 1974.

Lay, T., and D.V. Helmberger, A lower mantle S-wave triplication and the velocity structure of D", *Geophys. J., 75,* 799-837, 1983.

Mondt, J.C., SH waves: theory and observations for epicentral distances greater than 90°, *Phys. Earth Plan. Int., 15,* 46-59, 1977.

Morelli, A., and A.M. Dziewonski, 3D structure of the earth's core inferred from travel time residuals (abstract), *Eos, Trans. AGU, 67,* 311, 1986.

Mula, A.H., and G. Müller, Ray parameters of diffracted long period P and S waves and the velocities at the base of the mantle, *PAGEOPH, 118,* 1270-1290, 1980.

Woodhouse, J.H., and A. M. Dziewonski, Mapping the upper mantle: Three-dimensional modeling of Earth structure by inversion of seismic waveforms, *J. Geophys. Res., 89,* 5953-5986, 1984.

Wysession, M., and E. Okal, Evidence for lateral heterogeneity at the core-mantle boundary from the slowness of diffracted S profiles, in *Structure and Dynamics of Earth's Deep Interior, AGU Monog. 46,* p. 55-63, 1988.

Michael E. Wysession and Emile A. Okal, Department of Geological Sciences, Northwestern University, Evanston, Illinois 60208.

(Received August 14, 1989;
Accepted September 18, 1989.)